

Yixu Zong

Department of Materials Science and Engineering, Cornell University, Ithaca, NY 14850 e-mail: yz2339@cornell.edu

Pongkarn Chakthranont

National Nanotechnology Center (NANOTEC), National Science and Technology Development Agency (NSTDA), Pathum Thani 12120, Thailand e-mail: Pongkarn.cha@nanotec.or.th

Jin Suntivich

Department of Materials Science and Engineering, Kayli Institute at Cornell for Nanoscale Science. Cornell University, Ithaca, NY 14853 e-mail: jsuntivich@cornell.edu

Temperature Effect of CO₂ **Reduction Electrocatalysis on Copper: Potential Dependency** of Activation Energy

The electrochemical CO₂ reduction reaction (CO₂RR) has gathered widespread attention in the past decade as an enabling component to energy and fuel sustainability. Copper (Cu) is one of the few electrocatalysts that can convert CO_2 to higher-order hydrocarbons. We report the CO₂RR on polycrystalline Cu from 5 °C to 45 °C as a function of electrochemical potential. Our result shows that selectivity shifts toward CH_4 at low temperature and H_2 at high temperature at the potential values between -0.95 V and -1.25 V versus reversible hydrogen electrode (RHE). We analyze the activation energy for each product and discuss the possible underlying mechanism based on their potential dependence. The activation barrier of CH₄ empirically obeys the Butler-Volmer equation, while C₂H₄ and CO show a non-trivial trend. Our result suggests that the CH₄ production proceeds via a classical electrochemical pathway, likely the proton-coupled electron transfer of surface-saturated CO_{ad} , while C_2H_4 is limited by a more complex process, likely involving surface adsorbates. Our measurement is consistent with the view that the adsorbate-adsorbate interaction dictates the C_{2+} selectivity. [DOI: 10.1115/1.4046552]

Keywords: electrocatalysis, electrochemical energy storage, electrokinetics, electrofuels, electrolyzers

1 Introduction

The mitigation of atmospheric carbon dioxide (CO₂) via carbon capture and storage is an essential component of the global effort to combat climate changes [1,2]. Several CO₂ capture and storage strategies have been discussed and reported to date, for example, by using minerals or an underground geological formation as a storage facility [3,4]. While these approaches could lead to a carbon storage option, an alternative is to use renewable electricity to electrochemically convert captured CO2 to high-valued molecules such as CO and hydrocarbons [5–9]. Intrigued by this possibility, there has been an intense search for an electrocatalyst that can facilitate the CO₂ reduction reaction (CO₂RR) selectively and efficiently [10-15]. Cu is one of the few electrocatalysts that can electro-convert CO_2 to C_{2+} hydrocarbons [16–18]. However, Curequires high overpotential (>1.0 V) and suffers from poor selectivity due to the concurrent occurrence of the hydrogen evolution reaction (HER).

To improve the CO₂RR activity and selectivity, researchers have investigated the CO₂RR mechanism to find the rate-limiting process. Based on the studies of model electrocatalysts [19], electrochemical potential [20-22], reaction condition, e.g., electrolyte [23-25], pressure [26,27], temperature [28-30]), and electrodeelectrolyte configuration [31-33], the current view is that the active species (H2O for HER and CO2 for CO2RR) compete for surface adsorption, where the adsorbate-adsorbate interactions (e.g., CO-CO and CO₂-H) control selectivity [34-37]. With regards to the competition between CH₄ and C₂H₄, Schouten et al. suggest that CH₄ forms via the concerted proton-electron transfer mechanism, while C₂H₄ occurs via the protonation of the CO dimer [38,39]. In this picture, the CH₄ rate is governed by an electrochemical step that is coupled to proton transfer (i.e., pH-invariant at constant overpotential versus reversible hydrogen electrode, RHE), while C₂H₄ is governed by an electrochemical step that is proton-independent (i.e., pH-invariant at constant overpotential versus vacuum-based reference).

As part of an effort to provide references for the studies of CO₂RR and factors controlling selectivity, we present our temperature-dependent measurement of the CO₂RR on Cu from 5 °C to 45 °C. From the perspective of temperature, Hori et al. have reported reduced Faradaic efficiencies (FE) for H₂, C₂H₄, and CO and increased FE for CH₄ with decreasing temperature (from 40 °C to 0 °C) [29]. However, because the selectivity was reported only at one fixed current (at 5 mA/cm²), it is not straightforward to extract the activation energy for each CO₂RR product. Recently, Ahn et al. reported the CO₂RR on Cu from 2 °C to 42 °C at a fixed potential (-1.6 V versus Ag/AgCl) [30]. Similar to Hori et al., Ahn et al. found that lower temperatures increased CH₄ and lowered HER, a notable finding given that Hori et al. and Ahn et al. used different CO₂RR conditions (0.5M KHCO₃ in the former and 0.1M KHCO₃ in the latter). However, there is not yet an effort to measure the temperature dependence of the CO₂RR as a function of electrochemical potential to obtain the activation energy (E_a) and its dependence on overpotential.

In this work, we investigate the activation energy in the CO₂RR and how they depend on overpotential to reveal insights into the nature of the rate-limiting process in the CO₂RR. Because the CO₂RR results are a complex function of intrinsic electrochemical kinetics and transport, we emphasize that the activation energy reported is an "apparent" value. We do not intend to suggest that the obtained activation energy represents a specific molecular mechanism. Rather, our aim is to provide results that could be useful for future CO₂RR studies focusing on separating the influence of intrinsic kinetics versus mass transport. Lobaccaro et al. had recently discovered that high surface-area-to-electrolyte-volume ratios can indirectly influence the temperature of the CO₂RR device [40]. Directly measuring the role of temperature on the CO₂RR can therefore offer an additional resource to understand how the CO₂RR device functions in the limit where the operating condition cannot keep the system temperature constant.

Our measurement of the CO2RR on Cu and its temperature dependency spans a range of electrochemical potential. In addition

¹Corresponding author.

Manuscript received September 24, 2019; final manuscript received February 21, 2020; published online March 4, 2020. Assoc. Editor: Kyle Grew.

to studying selectivity, we analyze partial current densities and use their temperature dependence to obtain E_a for each gaseous product: CH₄, C₂H₄, CO, and H₂. Our measurement reveals that CH₄ has the lowest E_a and that its potential dependence obeys the Butler–Volmer form with the transfer coefficient α of -0.3, i.e., the overpotential application reduces the activation barrier. Surprisingly, HER, despite being the major product, has the highest E_a with a non-trivial potential dependence. We assess these results within the context of the current CO₂RR mechanistic hypothesis and discuss a possible route to improve future performance.

2 Experimental Methods

2.1 Copper Working Electrode Preparation. Polycrystal-line Cu foil (BTC, 0.1 mm thick, 99.9999%) was cut into 0.5 cm \times 0.5 cm pieces for preparation of the working electrode. A Ti wire was attached to each copper piece with Leitsilber 200 Ag paint (Ted Pella, Inc.) and dried for at least 2 h. After, both the Cu foil and the part of the Ti wire were covered by inert epoxy (Omegabond 101) except the 0.1 cm² test area and dried for a period of several days. Before each experiment, the Cu electrode was electropolished in 85% phosphoric acid (Sigma Aldrich) for 1 s at 1 A/cm² and rinsed thoroughly by 18.2 m Ω de-ionized water [14].

2.2 Electrochemical Characterization. A custom two-compartment cell (H-cell) with separated water circulation jackets was made for the temperature-dependent experiment. A Nafion[®] 117 membrane was used to separate the catholyte and anolyte chambers, which held 15 mL and 7 mL of 0.1M KHCO₃ electrolyte, respectively. CO₂ (Airgas, ultra-high purity) was introduced into the catholyte inner chamber for about 20 min at 20 mL/min before and at 1 mL/min during the CO₂RR measurement. The ratio of surface area (~0.25 cm²) to electrolyte volume (~15 cm³) is smaller than the value, where bulk CO₂ depletion was suggested to be problematic [40].

The electrochemical testing was conducted using a standard three-electrode system using a potentiostat (Bio-Logic SP-300). The counter electrode is a Pt wire placed into the anolyte chamber, while the reference electrode is a Ag/AgCl counter placed in the catholyte chamber together with the working Cu electrode. We set the potentiostat compensation at the 85% value of the uncompensated resistance. The remaining 15% was post-corrected manually. This setting was found to provide the most accurate and reproducible potential control. The Ag/AgCl reference was calibrated by measuring the equilibrium potential of H₂ redox on a polycrystalline Pt disk (Pine) in H₂ (Airgas, ultra-high purity) in the 0.1M KHCO₃ electrolyte. We note that this calibration is only an approximation to RHE since the H₂ purging removes CO₂ from the solution, which should theoretically influence pH. We used a software (VISUAL MINTEQ ver. 3.1) to model the CO₂-carbonatepotassium equilibria at fixed ionic concentration and found that this effect is small (<30 mV) [41]. We measured 0 V versus RHE as $-616\,\mathrm{mV}$ versus Ag/AgCl at $5\,^\circ\mathrm{C}$, $-609\,\mathrm{mV}$ versus Ag/AgCl at 15 °C, -601 mV at 25 °C, -593 mV at 35 °C, and -584 mV at 45 °C.

During the experiment, the outer jacket of the cell was connected to a refrigeration and a heating circulator (Julabo, Model F25-ME), where the temperature-controlled water was circulated to maintain the desired temperature in the testing cell. The inner chamber was directly coupled to the gas chromatography (GC) through a rubber stopper connection. The inner chamber temperature was monitored via a temperature sensor. The temperature difference between the inner chamber and the set temperature was less than $0.5\,^{\circ}\text{C}$. We found no difference whether CO_2 was bubbled during the ramp time or after the electrolyte reached the set temperature.

2.3 Product Quantification. A GC (SRI) equipped with a thermal conductivity detector and flame ionization detector (FID) was used to quantify the gas product using Ar carrier gas (Airgas,

ultra-high purity). A hydrogen generator (H₂-100, SRI) was used for the FID carrier production. Gas was sampled from the reaction vessel 20 min after applying the overpotential, which spent 20 min to separate through the GC columns with a 10 min rest. Two samples were subsequently measured in 30 min interval such that the total experimental time was 1 h for each working electrode. The FE was calculated by dividing the charges required to produce each product by the total charge transferred during the time of the GC sampling. We reproduced the measurements three times, represented through the standard deviations in the obtained results.

3 Results and Discussions

To ensure the working of the temperature-controlled electrochemical cell, we first measured the CO_2RR on Cu at room temperature (25 °C) between -0.85 V and -1.20 V versus RHE. Figure 1 shows the results for our temperature-dependent cell. The CO_2RR result is consistent with the previously reported data [20]. This measurement gave us confidence in proceeding to the temperature-dependent experiment, where we tested at 5 °C, 15 °C, 35 °C, and 45 °C for the gaseous products of the CO_2RR : CH_4 , CO, C_2H_4 , and H_2 (Fig. 2).

Our measurement reveals that the CH_4 selectivity increases at lower temperatures for all potentials. At 5 °C, CH_4 approaches the FE of 60.5% at -1.20 V versus RHE compared to 37.35% at 25 °C. In contrast, H_2 dominates the product distribution at higher temperatures. At 45 °C, the FE of H_2 is greater than 55% at all potentials, whereas the FE of CH_4 is smaller than 20%. The CO selectivity is slightly higher at 35 °C and 45 °C in comparison to lower temperatures at more negative overpotentials (>-1.05 V versus RHE). The temperature effect on the C_2H_4 does not show a straightforward trend.

Several researchers have reported that temperature can affect the CO_2 solubility in aqueous solutions [40,42,43]. Thus, the simplest explanation for the observed CO_2RR selectivity reduction is the reduced CO_2 solubility at higher temperatures (35 °C and 45 °C). On the other hand, the increased CO_2 solubility at lower temperatures (5 °C, 15 °C, and 25 °C) positively impacts the CO_2RR selectivity. This explanation is consistent with the observed increase in the CO_2RR selectivity. However, the CO_2 solubility is unlikely the only effect; if CO_2 solubility was the only reason, we would expect the partial current densities to decrease with temperature (as it would scale with the CO_2 concentration). Instead, we observe that the partial current densities increase with temperature for all products despite the reduced CO_2 availability (Fig. 3). We,

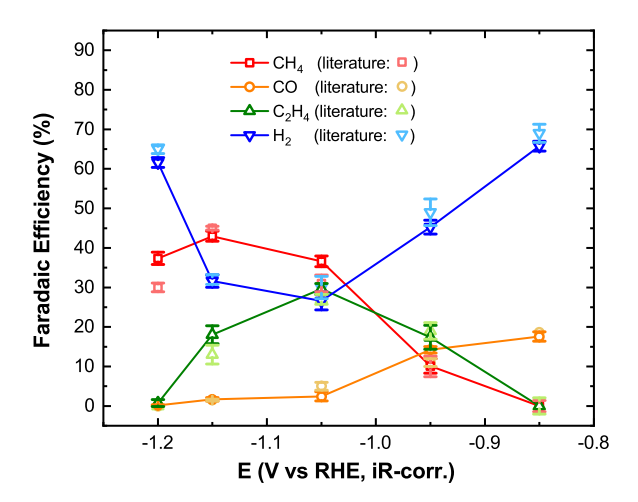


Fig. 1 Faradaic efficiencies of the CO_2RR gaseous products in the temperature-controlled cell in comparison to an example literature result [20]. The experiment was tested using polycrystal-line Cu in CO_2 saturated 0.1M KHCO₃ at 25 °C.

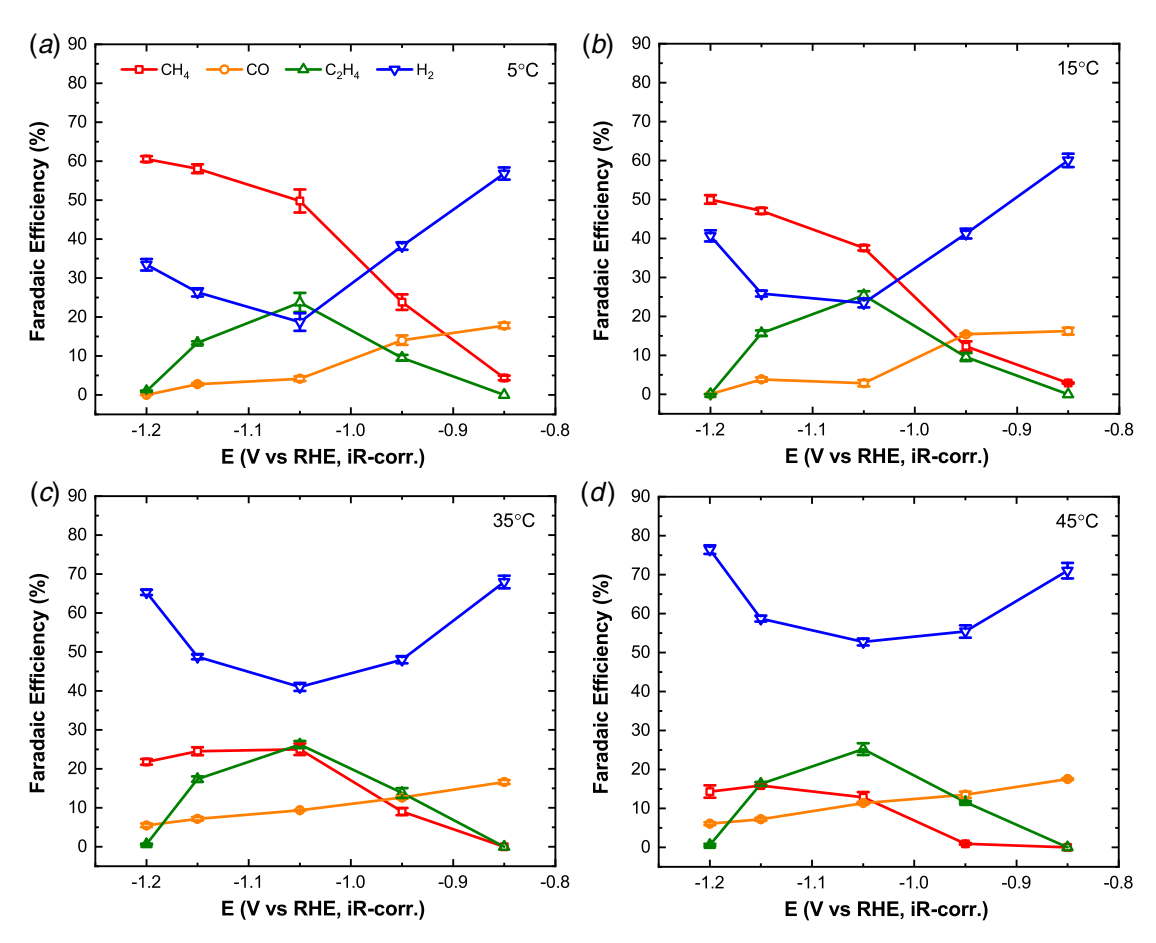


Fig. 2 Faradaic efficiencies of the CO₂RR gaseous products in the temperature-controlled cell. The experiment was tested using polycrystalline Cu in CO₂ saturated 0.1M KHCO₃ at (a) 5 °C, (b) 15 °C, (c) 35 °C, and (d) 45 °C.

therefore, suspect that temperature also affects the electrochemical kinetics in addition to mass transport (CO_2 solubility). To better understand these effects, we measure the activation energy for each product.

We conducted an Arrhenius analysis by examining the logarithmic dependence of the partial current density with inverse temperature. The total current density was obtained by averaging the reduction current over 1 h and normalized by the electrode area, which can be subsequently multiplied by the FE to get the corresponding partial current density for each product. Figure 3 shows the Arrhenius plots for CH₄, C₂H₄, CO, and H₂. For each product, we plotted at four fixed potentials -0.95, -1.05, -1.15, and -1.20 V versus RHE. We applied a linear fit to the logarithm form of the Arrhenius equation:

$$\ln(i) = -\frac{E_a}{R} \left(\frac{1}{T}\right) + \ln(A) \tag{1}$$

where $E_{\rm a}$ is the activation energy, A is the pre-exponential factor, and a is the "rate constant."

As shown in Fig. 4, the activation barrier (E_a) of CH_4 decreases with increasing overpotential. This result suggests that the rate-limiting step of CH_4 is likely an electrochemical process or a chemical process that involves an electrochemical pre-equilibrium. On the zero-order approximation, mass transport of neutral species is independent of potential [44]. In this approximation, CH_4 appears to not be limited by mass transport of neutral species such as CO_2 . We emphasize that this does not mean that mass transport is not critical; increasing the concentration of reactive species at the electrode–electrolyte interface will impact both the electrochemical

process and the chemical step involved in the pre-equilibrium process. Our analysis only suggests that the $\mathrm{CH_4}$ production does not appear to be solely limited by the mass transport in the studied condition. We caution that there could also be the higher-order effect of potential-transport coupling, e.g., electro-osmotic drag [45]. Understanding this effect is beyond the scope of our current work.

In the comparison, the activation energy for CO is potential independent except at -0.95 V versus RHE, where the activation energy changes from 28 kJ/mol (-0.95 V versus RHE) to 52 kJ/mol (-1.05 V versus RHE). The activation energy for H₂ follows a similar trend as CO, which may indicate that both reactions follow a similar catalysis pathway. Interestingly, the activation energy of HER is consistently the highest, despite H₂ being a major product. This observation indicates that HER kinetics must have a larger prefactor, i.e., ln(A) in Eq. (1), than the CO_2RR . We speculate that the large pre-factor is related to the facile nature of the elementary process involved in the rate-limiting step of the HER or to the availability of the active centers. In the former, the large abundance of water, the reactant of the HER, can drive up the reaction kinetics via the reaction order effect. In the latter, there could be more HERactive sites than the ones responsible for CO₂RR. Cu(211) and Cu(111) are more efficient for the CH₄ production [46-49], whereas Cu(100) is more efficient for the C₂H₄ production [13,38,39,48]. Assuming that most Cu terrace atoms are active for the HER, there are more Cu sites that are responsible for the HER than for each specific CO₂RR product. As a result, the HER has a larger pre-factor value than the CO₂RR. We note that active centers for the CO₂RR could also be the minority grain-boundary atoms [50], which would also be consistent with our observation.

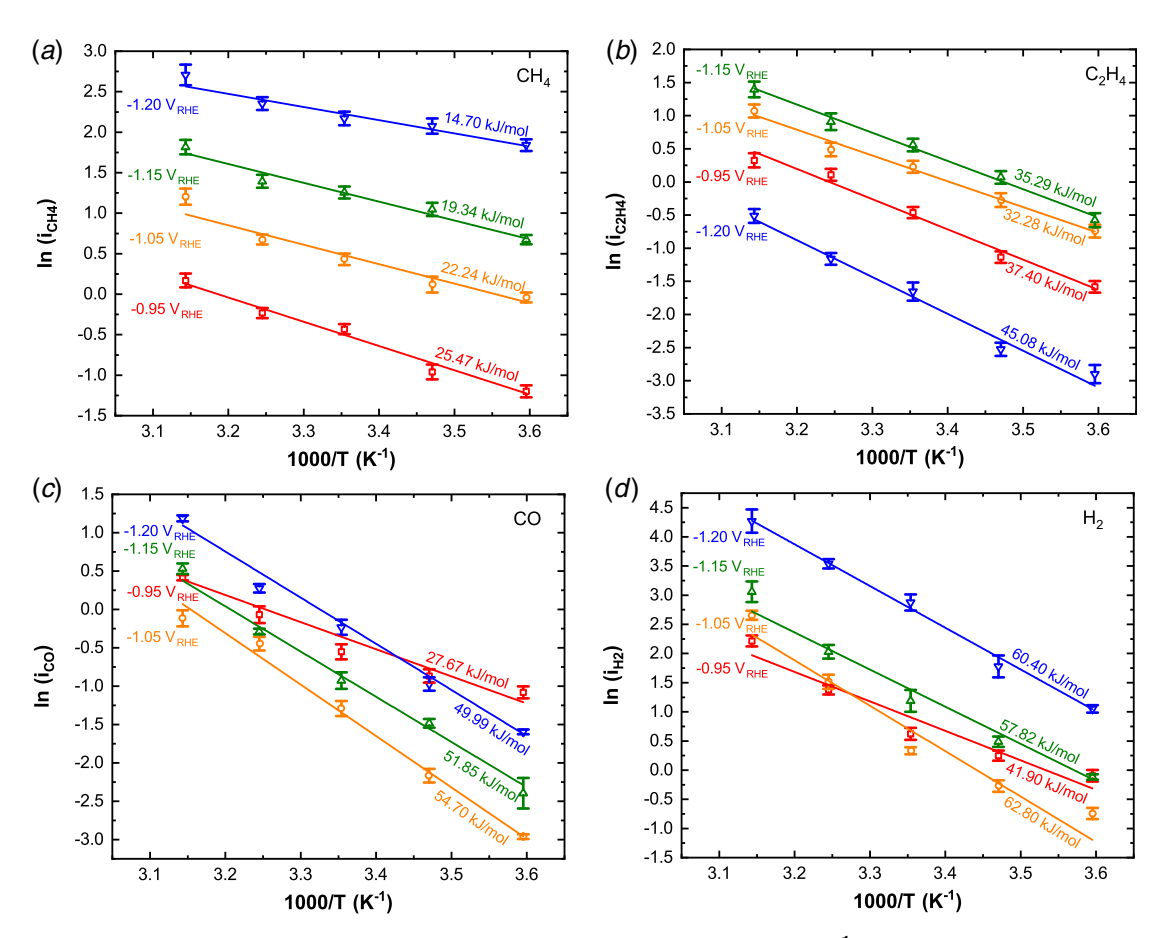


Fig. 3 Arrhenius plots for (a) CH₄, (b) C₂H₄, (c) CO, (d) H₂. Log(activity) versus T^{-1} at -0.95 V, -1.05 V, -1.15 V, and -1.20 V versus RHE. Fitted E_a are shown next to the lines.

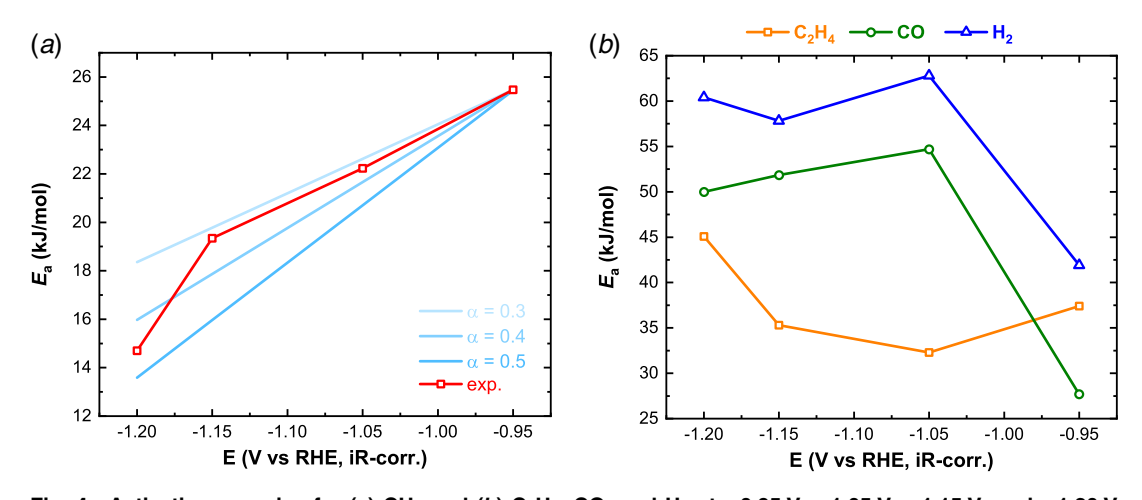


Fig. 4 Activation energies for (a) CH₄ and (b) C_2H_4 , CO, and H_2 at -0.95 V, -1.05 V, -1.15 V, and -1.20 V versus RHE. In (a), results for transfer coefficients of 0.3, 0.4, and 0.5 are shown as references.

We can use the Butler–Volmer equation to quantify the relationship between the CO_2RR kinetics, the activation energy, and the electrochemical driving force. The Butler–Volmer equation in the limit of large overpotential, η , where we can neglect the backward term, is

$$\frac{\partial}{\partial (1/T)} \ln(i) = \frac{\partial}{\partial (1/T)} \ln(i_0) - \frac{\alpha F}{R} \cdot \eta \tag{2}$$

In an ideal situation, the exchange current density, i_0 , is independent of η . However, for surface electrochemical reactions, i_0 may

depend on η since the surface concentration of reacting species may be potential dependent. We will discuss this possibility later. First, we use the temperature dependence of $E_{\rm a}$ from Eq. (1) and connect the result to the Butler–Volmer equation, i.e., Eq. (2):

$$-\frac{E_{\rm a}}{R} = \frac{\partial}{\partial (1/T)} \ln(i_0) - \frac{\alpha F}{R} \cdot \eta \tag{3}$$

Figure 4(*a*) shows the relationship between the activation energy and potential for CH₄. The approximation of the linearity matches well to $\alpha \sim 0.3$ except for the data point at -1.2 V versus RHE.

The α value from the temperature-dependency analysis agrees well with the α value obtained by fitting the Butler–Volmer equation directly to the potential dependence of the CH₄ partial current density (Fig. 5). Notably, the Butler–Volmer fit to the partial current density of CH₄ reveals α to range from 0.25 to 0.29, depending on the temperature used. Our result unambiguously shows that the CO₂RR pathway toward CH₄ obeys the Butler–Volmer kinetics between –0.95 V and –1.15 V versus RHE, with i_0 exhibiting negligible potential dependence and with α ~ 0.3.

As discussed earlier, the CH₄ production is a surface electrochemical reaction. The observation that $\ln i$ versus T^{-1} is linear implies that the relevant surface species for the CH₄ production does not depend on the electrochemical potential in the experimental condition studied. Peterson et al. suggested that the CO hydrogenation ($CO_{ad} + H^+ + e^- \rightarrow COH_{ad}$) is the potential-determining step for the CH₄ production based on the thermodynamic analysis using the density functional theory (DFT) [46]. Our observation suggests that the surface CO_{ad} population is potential invariant at <-0.95 V versus RHE, which is consistent with Wuttig et al. [51]. Our potential-independent i_0 finding is thus a result of the weak dependence of the CO_{ad} concentration on the electrochemical potential in the studied potential range.

We next discuss the activation energy for the HER. We began by pointing out that the HER activation energy is nearly potential independent, with the exception at -0.95 V versus RHE, where the activation energy increases as potential decreases. Many firstprinciple calculations have suggested that the formation of the HER intermediate (H_{ad}) is thermodynamically spontaneous at -0.95 V versus RHE [36,37]. We thus speculate that the ratelimiting step of the HER may not be electrochemical in nature at this potential. One possibility is that the water dissociation step controls the HER on Cu at this potential. Strmcnik and co-workers have suggested that water dissociation may be the rate-limiting step of the HER in alkaline [52]. If this situation occurs on Cu, the water dissociation may be a chemical step at the studied overpotential. Interestingly, the activation energy for the HER (~40–60 kJ/mol) is comparable to the water dissociation energy, which we estimate by subtracting the water dissociation energy (~106-125 kJ/mol [53]) from the adsorption energy (\sim 34–60 kJ/mol [54]). We caution that this is a crude approximation and more detailed studies are necessary to reveal the connection between water adsorption and HER. The primary challenge limiting our activation energy analysis is the complexity of the interactions between the adsorbates that are the intermediates of the HER and CO₂RR. Nonetheless, it is interesting to note that the water dissociation process has also been suggested to play an important role in the water-gas shift reaction [55,56].

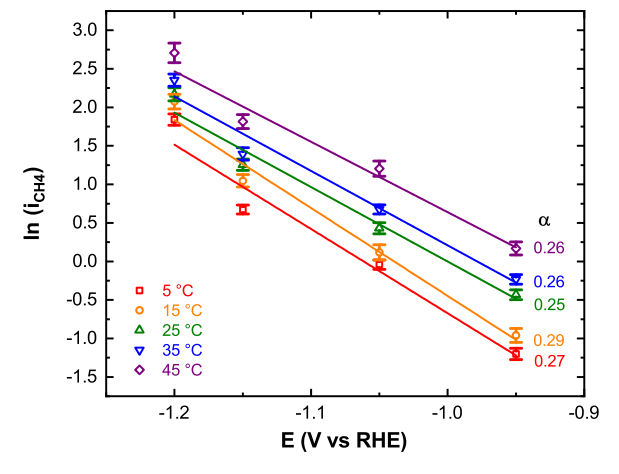


Fig. 5 Extracted transfer coefficient α from the Butler–Volmer fitting to the CH₄ production at different temperatures. We found α to range from 0.26 to 0.29.

The relationship between the activation energy and electrochemical potential for the CO production is similar to H_2 (Fig. 4(b)). Notably, E_a is constant for CO with the lone exception at -0.95 V versus RHE, where the activation energy increases as the potential decreases. Since CO is both a product and a reactant, the observed E_a is convoluted by the possibility that the produced CO_{ad} can be detached as free CO or consumed for the subsequent CO_2RR steps [57]. We hypothesize that the CO_{ad} desorption is the rate-limiting step of the CO production. We support this hypothesis by pointing out that the measured activation energy (\sim 50–55 kJ/mol) is comparable to the CO adsorption energies on Cu (\sim 47–58 kJ/mol [58]) except at -0.95 V versus RHE, which has lower E_a (\sim 27 kJ/mol). The origin of the lower E_a at -0.95 V versus RHE is unclear at present.

For C₂H₄, the activation energy also remains largely constant. Schouten et al. reported that the C₂H₄ pathway occurs via the protonation of the CO dimer [38,39]. We believe that the observed potential independence of E_a suggests that the rate-limiting step at -0.95 V versus RHE is a chemical step, for example, the dimerization of CO_{ad} prior to the protonation of the CO dimer. Comparing to the DFT result by Montoya et al., our observed activation energy (30–45 kJ/mol, i.e., 0.3–0.45 eV) is comparable to the computed energy of the CO dimerization process (0.33 eV on Cu(100) [59]). Thus, this simple interpretation is consistent with our result, although a more realistic model that captures the interfacial complexity would be critical to improving the mechanistic understanding in the future. Understanding surface adsorbate dynamics, in particular, how they compete for space and selectivity is likely the key to enhancing our CO₂RR understanding, including the use of modeling to track the CO_{ad} generation, adsorption, and consumption. We hope that the data provided herein can be used as a benchmark to test the model, as the community moves closer to unraveling the CO₂RR mechanism.

4 Conclusion

We have shown that decreasing temperature can suppress the HER and increase the CO2RR selectivity toward CH4 in the range of -0.95 V to −1.20 V versus RHE, a commonly used electrochemical potential window for CO₂RR studies. The activation energy versus overpotential analysis reveals that the CH₄ production obeys the Butler-Volmer expression, where the overpotential application decreases the activation energy. This finding suggests that CH₄ is limited by an electrochemical process that involves surface species that does not change with potential, likely CO_{ad}. In comparison, the activation energy of C₂H₄ and H₂ exhibit weak potential dependence, which implies that their limiting steps could be chemical, for example, CO dimerization for the former and water dissociation for the latter. Interestingly, HER has the highest activation barrier of all products despite being one of the most significant products. This finding implies that there are more HER-active surface species (such as H_{ad}) than the CO₂RR species. Our work provides reference data for the temperature dependence of the CO₂RR and offers mechanistic insight into how the gaseous products originate from the CO₂RR on Cu. The temperature-dependent technique and the presented activation energy analysis could be adapted to study other catalytic materials in the future.

Acknowledgment

We thank Kevin Fritz, Emily Nishiwaki, Zhichu Tang, Kevin Kimura, and Tobias Hanrath for their help with the $\rm CO_2RR$ experiment and its interpretation. This material is based upon work supported by the National Science Foundation (NSF) under Grant No. CBET-1805400.

References

 Chu, S., 2009, "Carbon Capture and Sequestration," Science, 325(5948), pp. 1599.

- [2] Figueroa, J. D., Fout, T., Plasynski, S., McIlvried, H., and Srivastava, R. D., 2008, "Advances in CO₂ Capture Technology—The US Department of Energy's Carbon Sequestration Program," Int. J. Greenhouse Gas Control, 2(1), pp. 9–20.
- [3] Boot-Handford, M. E., Abanades, J. C., Anthony, E. J., Blunt, M. J., Brandani, S., Mac Dowell, N., Fernandez, J. R., Ferrari, M. C., Gross, R., Hallett, J. P., Haszeldine, R. S., Heptonstall, P., Lyngfelt, A., Makuch, Z., Mangano, E., Porter, R. T. J., Pourkashanian, M., Rochelle, G. T., Shah, N., Yao, J. G., and Fennell, P. S., 2014, "Carbon Capture and Storage Update," Energy Environ. Sci., 7(1), pp. 130–189.
- [4] Anderson, S., and Newell, R., 2004, "Prospects for Carbon Capture and Storage Technologies," Annu. Rev. Environ. Resour., 29(1), pp. 109–142.
- [5] Song, C., 2006, "Global Challenges and Strategies for Control, Conversion and Utilization of CO₂ for Sustainable Development Involving Energy, Catalysis, Adsorption and Chemical Processing," Catal. Today, 115(1–4), pp. 2–32.
- [6] Kondratenko, E. V., Mul, G., Baltrusaitis, J., Larrazábal, G. O., and Pérez-Ramírez, J., 2013, "Status and Perspectives of CO₂ Conversion Into Fuels and Chemicals by Catalytic, Photocatalytic and Electrocatalytic Processes," Energy Environ. Sci., 6(11), pp. 3112–3135.
- [7] Dubois, M. R., and Dubois, D. L., 2009, "Development of Molecular Electrocatalysts for CO₂ Reduction and H₂ Production/Oxidation," Acc. Chem. Res., 42(12), pp. 1974–1982.
- [8] Chen, C., Kotyk, J. F. K., and Sheehan, S. W., 2018, "Progress Toward Commercial Application of Electrochemical Carbon Dioxide Reduction," Chem, 4(11), pp. 2571–2586.
- [9] Smith, W. A., Burdyny, T., Vermaas, D. A., and Geerlings, H., 2019, "Pathways to Industrial-Scale Fuel Out of Thin Air From CO₂ Electrolysis," Joule, 3(8), pp. 1822–1834.
- [10] Gattrell, M., Gupta, N., and Co, A., 2006, "A Review of the Aqueous Electrochemical Reduction of CO₂ to Hydrocarbons at Copper," J. Electroanal. Chem., 594(1), pp. 1–19.
- [11] Lu, Q., Rosen, J., Zhou, Y., Hutchings, G. S., Kimmel, Y. C., Chen, J. G. G., and Jiao, F., 2014, "A Selective and Efficient Electrocatalyst for Carbon Dioxide Reduction," Nat. Commun., 5, p. 6.
- [12] Sheng, W., Kattel, S., Yao, S., Yan, B., Liang, Z., Hawxhurst, C. J., Wu, Q., and Chen, J. G., 2017, "Electrochemical Reduction of CO₂ to Synthesis Gas With Controlled CO/H₂ Ratios," Energy Environ. Sci., 10(5), pp. 1180–1185.
- [13] Roberts, F. S., Kuhl, K. P., and Nilsson, A., 2015, "High Selectivity for Ethylene From Carbon Dioxide Reduction Over Copper Nanocube Electrocatalysts," Angew. Chem. Int. Ed., 54(17), pp. 5179–5182.
- [14] Hall, A. S., Yoon, Y., Wuttig, A., and Surendranath, Y., 2015, "Mesostructure-Induced Selectivity in CO₂ Reduction Catalysis," J. Am. Chem. Soc., 137(47), pp. 14834–14837.
- [15] Schreier, M., Luo, J., Gao, P., Moehl, T., Mayer, M. T., and Grätzel, M., 2016, "Covalent Immobilization of a Molecular Catalyst on Cu₂O Photocathodes for CO₂ Reduction," J. Am. Chem. Soc., 138(6), pp. 1938–1946.
- [16] Kuhl, K. P., Cave, E. R., Abram, D. N., and Jaramillo, T. F., 2012, "New Insights Into the Electrochemical Reduction of Carbon Dioxide on Metallic Copper Surfaces," Energy Environ. Sci., 5(5), pp. 7050–7059.
 [17] Li, C. W., and Kanan, M. W., 2012, "CO₂ Reduction at Low Overpotential on Cu
- Electrodes Resulting From the Reduction of Thick Cu₂O Films," J. Am. Chem. Soc., **134**(17), pp. 7231–7234.
- [18] Y. Hori, 2008, "Electrochemical CO₂ Reduction on Metal Electrodes," *Modern Aspects of Electrochemistry*, Vol. 42, C. G. Vayenas, R. E. White, and M. E. Gamboa-Aldeco, eds., Springer, New York, pp. 89–189.
- [19] Ma, M., Djanashvili, K., and Smith, W. A., 2016, "Controllable Hydrocarbon Formation From the Electrochemical Reduction of CO₂ Over Cu Nanowire Arrays," Angew. Chem. Int. Ed., 55(23), pp. 6680–6684.
- [20] Kimura, K. W., Fritz, K. E., Kim, J., Suntivich, J., Abruna, H. D., and Hanrath, T., 2018, "Controlled Selectivity of CO₂ Reduction on Copper by Pulsing the Electrochemical Potential," ChemSusChem, 11(11), pp. 1781–1786.
- [21] Kumar, B., Brian, J. P., Atla, V., Kumari, S., Bertram, K. A., White, R. T., and Spurgeon, J. M., 2016, "Controlling the Product Syngas H₂:CO Ratio Through Pulsed-Bias Electrochemical Reduction of CO₂ on Copper," ACS Catal., 6(7), pp. 4739–4745.
- [22] Engelbrecht, A., Uhlig, C., Stark, O., Hammerle, M., Schmid, G., Magori, E., Wiesner-Fleischer, K., Fleischer, M., and Moos, R., 2018, "On the Electrochemical CO₂ Reduction at Copper Sheet Electrodes With Enhanced Long-Term Stability by Pulsed Electrolysis," J. Electrochem. Soc., 165(15), pp. J3059–J3068.
- [23] Varela, A. S., Kroschel, M., Reier, T., and Strasser, P., 2016, "Controlling the Selectivity of CO₂ Electroreduction on Copper: The Effect of the Electrolyte Concentration and the Importance of the Local pH," Catal. Today, 260, pp. 8–13.
- [24] Murata, A., and Hori, Y., 1991, "Product Selectivity Affected by Cationic Species in Electrochemical Reduction of CO₂ and CO at a Cu Electrode," Bull. Chem. Soc. Jpn, 64(1), pp. 123–127.
- [25] Matsubara, Y., Grills, D. C., and Kuwahara, Y., 2015, "Thermodynamic Aspects of Electrocatalytic CO₂ Reduction in Acetonitrile and With an Ionic Liquid as Solvent or Electrolyte," ACS Catal., 5(11), pp. 6440–6452.
 [26] Hara, K., Kudo, A., and Sakata, T., 1995, "Electrochemical Reduction of Carbon
- [26] Hara, K., Kudo, A., and Sakata, T., 1995, "Electrochemical Reduction of Carbon Dioxide Under High Pressure on Various Electrodes in an Aqueous Electrolyte," J. Electroanal. Chem., 391(1–2), pp. 141–147.
- [27] Kaneco, S., Iiba, K., Katsumata, H., Suzuki, T., and Ohta, K., 2006, "Electrochemical Reduction of High Pressure CO₂ at a Cu Electrode in Cold Methanol," Electrochim. Acta, 51(23), pp. 4880–4885.
- [28] Azuma, M., Hashimoto, K., Hiramoto, M., Watanabe, M., and Sakata, T., 1990, "Electrochemical Reduction of Carbon Dioxide on Various Metal Electrodes in

- Low-Temperature Aqueous KHCO₃ Media," J. Electrochem. Soc., **137**(6), pp. 1772–1778.
- [29] Hori, Y., Kikuchi, K., Murata, A., and Suzuki, S., 1986, "Production of Methane and Ethylene in Electrochemical Reduction of Carbon Dioxide at Copper Electrode in Aqueous Hydrogencarbonate Solution," Chem. Lett., 15(6), pp. 897–898.
- [30] Ahn, S. T., Abu-Baker, I., and Palmore, G. T. R., 2017, "Electroreduction of CO₂ on Polycrystalline Copper: Effect of Temperature on Product Selectivity," Catal. Today, 288, pp. 24–29.
- [31] Hara, K., Kudo, A., Sakata, T., and Watanabe, M., 1995, "High Efficiency Electrochemical Reduction of Carbon Dioxide Under High Pressure on a Gas Diffusion Electrode Containing Pt Catalysts," J. Electrochem. Soc., 142(4), pp. L57–L59.
- [32] Higgins, D., Hahn, C., Xiang, C., Jaramillo, T. F., and Weber, A. Z., 2019, "Gas-Diffusion Electrodes for Carbon Dioxide Reduction: A New Paradigm," ACS Energy Lett., 4(1), pp. 317–324.
- [33] Sen, S., Leonard, M., Radhakrishnan, R., Snyder, S., Skinn, B., Wang, D., Hall, T., Taylor, E. J., and Brushett, F. R., 2018, "Pulse Plating of Copper Onto Gas Diffusion Layers for the Electroreduction of Carbon Dioxide," MRS Adv., 3(23), pp. 1277–1284.
- [34] Nitopi, S., Bertheussen, E., Scott, S. B., Liu, X., Engstfeld, A. K., Horch, S., Seger, B., Stephens, I. E. L., Chan, K., Hahn, C., Nørskov, J. K., Jaramillo, T. F., and Chorkendorff, I., 2019, "Progress and Perspectives of Electrochemical CO₂ Reduction on Copper in Aqueous Electrolyte," Chem. Rev., 119(12), pp. 7610–7672.
- [35] Sebastian-Pascual, P., Mezzavilla, S., Stephens, I. E. L., and Escudero-Escribano, M., 2019, "Structure-Sensitivity and Electrolyte Effects in CO2 Electroreduction: From Model Studies to Applications," ChemCatChem., 11(16), pp. 3626–3645.
- [36] Zhang, Y. J., Sethuraman, V., Michalsky, R., and Peterson, A. A., 2014, "Competition Between CO₂ Reduction and H₂ Evolution on Transition-Metal Electrocatalysts," ACS Catal., 4(10), pp. 3742–3748.
- [37] Cave, E. R., Shi, C., Kuhl, K. P., Hatsukade, T., Abram, D. N., Hahn, C., Chan, K., and Jaramillo, T. F., 2018, "Trends in the Catalytic Activity of Hydrogen Evolution During CO₂ Electroreduction on Transition Metals," ACS Catal., 8(4), pp. 3035–3040.
- [38] Schouten, K. J. P., Kwon, Y., van der Ham, C. J. M., Qin, Z., and Koper, M. T. M., 2011, "A New Mechanism for the Selectivity to C-1 and C-2 Species in the Electrochemical Reduction of Carbon Dioxide on Copper Electrodes," Chem. Sci., 2(10), pp. 1902–1909.
- [39] Schouten, K. J. P., Qin, Z. S., Gallent, E. P., and Koper, M. T. M., 2012, "Two Pathways for the Formation of Ethylene in CO Reduction on Single-Crystal Copper Electrodes," J. Am. Chem. Soc., 134(24), pp. 9864–9867.
- [40] Lobaccaro, P., Singh, M. R., Clark, E. L., Kwon, Y., Bell, A. T., and Ager, J. W., 2016, "Effects of Temperature and Gas-Liquid Mass Transfer on the Operation of Small Electrochemical Cells for the Quantitative Evaluation of CO₂ Reduction Electrocatalysts," Phys. Chem. Chem. Phys., 18(38), pp. 26777–26785.
- [41] Gustafsson, J. P., 2013, Visual MINTEQ version 3.1, Online, Stockholm, Sweden.
- [42] Zhong, H., Fujii, K., and Nakano, Y., 2016, "Electroactive Species Study in the Electrochemical Reduction of CO₂ in KHCO₃ Solution at Elevated Temperature," J. Energy Chem., 25(3), pp. 517–522.
- [43] De Jesús-Cardona, H., del Moral, C., and Cabrera, C. R., 2001, "Voltammetric Study of CO₂ Reduction at Cu Electrodes Under Different KHCO₃ Concentrations, Temperatures and CO₂ Pressures," J. Electroanal. Chem., 513(1), pp. 45–51.
- [44] Marković, N. M., Grgur, B. N., and Ross, P. N., 1997, "Temperature-Dependent Hydrogen Electrochemistry on Platinum Low-Index Single-Crystal Surfaces in Acid Solutions," J. Phys. Chem. B, 101(27), pp. 5405–5413.
- [45] Zawodzinski, T. A., Davey, J., Valerio, J., and Gottesfeld, S., 1995, "The Water Content Dependence of Electro-Osmotic Drag in Proton-Conducting Polymer Electrolytes," Electrochim. Acta, 40(3), pp. 297–302.
- [46] Peterson, A. A., Abild-Pedersen, F., Studt, F., Rossmeisl, J., and Nørskov, J. K., 2010, "How Copper Catalyzes the Electroreduction of Carbon Dioxide Into Hydrocarbon Fuels," Energy Environ. Sci., 3(9), pp. 1311–1315.
- [47] Nie, X., Esopi, M. R., Janik, M. J., and Asthagiri, A., 2013, "Selectivity of CO₂ Reduction on Copper Electrodes: The Role of the Kinetics of Elementary Steps," Angew. Chem. Int. Ed., 52(9), pp. 2459–2462.
- [48] Kortlever, R., Shen, J., Schouten, K. J. P., Calle-Vallejo, F., and Koper, M. T. M., 2015, "Catalysts and Reaction Pathways for the Electrochemical Reduction of Carbon Dioxide," J. Phys. Chem. Lett., 6(20), pp. 4073–4082.
- [49] Takahashi, I., Koga, O., Hoshi, N., and Hori, Y., 2002, "Electrochemical Reduction of CO₂ at Copper Single Crystal Cu(S)-n(111)x(111) and Cu(S)-n(110)x(100) Electrodes," J. Electroanal. Chem., 533(1-2), pp. 135-143.
- [50] Mariano, R. G., McKelvey, K., White, H. S., and Kanan, M. W., 2017, "Selective Increase in CO₂ Electroreduction Activity at Grain-Boundary Surface Terminations," Science, 358(6367), pp. 1187–1191.
- [51] Wuttig, A., Liu, C., Peng, Q., Yaguchi, M., Hendon, C. H., Motobayashi, K., Ye, S., Osawa, M., and Surendranath, Y., 2016, "Tracking a Common Surface-Bound Intermediate During CO₂-to-Fuels Catalysis," ACS Central Sci., 2(8), pp. 522–528.
- [52] Strmcnik, D., Lopes, P. P., Genorio, B., Stamenkovic, V. R., and Markovic, N. M., 2016, "Design Principles for Hydrogen Evolution Reaction Catalyst Materials," Nano Energy, 29, pp. 29–36.
- [53] Wang, Y. Q., Yan, L. F., and Wang, G. C., 2015, "Oxygen-Assisted Water Partial Dissociation on Copper: A Model Study," Phys. Chem. Chem. Phys., 17(12), pp. 8231–8238.
- [54] Tang, Q. L., and Chen, Z. X., 2007, "Density Functional Slab Model Studies of Water Adsorption on Flat and Stepped Cu Surfaces," Surf. Sci., 601(4), pp. 954–964.

- [55] Rodriguez, J. A., Liu, P., Wang, X., Wen, W., Hanson, J., Hrbek, J., Pérez, M., and Evans, J., 2009, "Water-Gas Shift Activity of Cu Surfaces and Cu Nanoparticles Supported on Metal Oxides," Catal. Today, 143(1–2), pp. 45–50.
- [56] Nakamura, J., Campbell, J. M., and Campbell, C. T., 1990, "Kinetics and Mechanism of the Water-Gas Shift Reaction Catalysed by the Clean and Cs-Promoted Cu(110) Surface: A Comparison With Cu(111)," J. Chem. Soc., Faraday Trans., 86(15), pp. 2725–2734.
- [57] Heyes, J., Dunwell, M., and Xu, B., 2016, "CO2 Reduction on Cu at Low Overpotentials With Surface-Enhanced in situ Spectroscopy," J. Phys. Chem. C, 120(31), pp. 17334–17341.
- [58] Vollmer, S., Witte, G., and Wéll, C., 2001, "Determination of Site Specific Adsorption Energies of CO on Copper," Catal. Lett., 77(1/3), pp. 97–101.
 [59] Montoya, J. H., Shi, C., Chan, K., and Nørskov, J. K., 2015, "Theoretical Insights
- [59] Montoya, J. H., Shi, C., Chan, K., and Nørskov, J. K., 2015, "Theoretical Insights Into a CO Dimerization Mechanism in CO₂ Electroreduction," J. Phys. Chem. Lett., 6(11), pp. 2032–2037.